Hepatology Research 2008; 38: 348–353 doi: 10.1111/j.1872-034X.2007.00280.x

Original Article

Evidence of oxidative stress as a cofactor in the development of insulin resistance in patients with chronic hepatitis C

Hironori Mitsuyoshi,[1] Yoshito Itoh,[1] Yoshio Sumida,[2] Masahito Minami,[1] Kouichirou Yasui,[1] Toshiaki Nakashima[3] and Takeshi Okanoue[4]

[1]*Molecular Gastroenterology and Hepatology, Graduate School of Medical Science, Kyoto Prefectural University of Medicine, Kyoto,* [2]*Department of Gastroenterology and Hepatology, Nara City Hospital, Nara,* [3]*Saiseikai Kyoto Hospital, Kyoto, and* [4]*Saiseikai Suita Hospital, Suita, Japan*

Aim: The mechanisms by which metabolic disorders develop in patients with chronic hepatitis C are unknown. Our study aimed to test whether oxidative stress contributes to these mechanisms.

Methods: The index of homeostasis model assessment–insulin resistance (HOMA–IR) and serum and hepatic levels of thioredoxin (Trx), which are markers of oxidative stress, were evaluated in 203 biopsy-proven chronic hepatitis C patients with hepatitis C virus (HCV) genotype 1 or 2 infection. HOMA–IR and Trx levels were compared with baseline values after phlebotomy in 23 patients.

Results: HOMA–IR and serum Trx levels were significantly correlated with disease stage (HOMA–IR, $P < 0.00001$; Trx, $P < 0.0001$) and independently predicted fibrosis scores (HOMA–IR, $P < 0.05$; Trx, $P < 0.005$). Steatosis (%) was significantly correlated with HOMA–IR ($P < 0.00005$) and Trx ($P < 0.001$) stage ($P < 0.00001$). Serum Trx levels were significantly correlated with HOMA–IR ($P < 0.05$), even after adjustment for body mass index ($P < 0.05$). Furthermore, the mRNA levels of hepatic Trx were significantly correlated with HOMA–IR ($P < 0.05$) and independently-predicted HOMA–IR ($P < 0.05$). The alanine aminotransferase ($P < 0.00001$), Trx ($P < 0.05$), and HOMA–IR ($P < 0.05$) serum levels decreased significantly after phlebotomy; these effects were similar even in non-responders to interferon.

Conclusion: Oxidative stress contributed to the development of IR irrespective of obesity in patients with HCV genotype 1 or 2 infection. This study could contribute to our understanding of how metabolic disorders develop and how they should be treated in chronic hepatitis C patients.

Key words: hepatitis C virus, insulin resistance, oxidative stress, steatosis, thioredoxin

INTRODUCTION

CHRONIC HEPATITIS C progresses to cirrhosis and eventually to hepatocellular carcinoma (HCC).[1] Although interferon (IFN)-based antiviral therapy has achieved great advances, it can not eradicate hepatitis C virus (HCV) in approximately 50% of patients infected with the genotype 1 strain,[1] which is highly prevalent in Japan. Therefore, other therapeutic strategies remain important, and efforts to understand the pathogenesis are required.

Metabolic disorders have recently been implicated in the pathogenesis of chronic hepatitis C.[2–6] HCV-infected patients with hepatic steatosis exhibit clinical features associated with metabolic syndromes,[3] and glucose intolerance is considered to represent an extra-hepatic manifestation of HCV infection.[2,4] Furthermore, grades of steatosis are reported to predict rapid fibrosis progression,[5] and diabetes increases the risk of HCC.[6] From these findings, insulin resistance (IR), a central cause of metabolic syndromes,[7] has been described as a risk factor in advanced staged chronic hepatitis C patients,[2,8] as seen in non-alcoholic steatohepatitis.[9] Thus, insulin signaling could be an important target for

Correspondence: Assistant Professor Hironori Mitsuyoshi, Molecular Gastroenterology and Hepatology, Graduate School of Medical Science, Kyoto Prefectural University of Medicine, Kamigyo-ku, Kyoto 602-8566, Japan. Email: hmitsu@koto.kpu-m.ac.jp
Received 20 June 2007; revision 3 September 2007; accepted 5 September 2007.

the management of patients with HCV infection; however, how IR develops is not well understood.

In this study, we focused on the role of oxidative stress, another key player in progressive liver injury in patients with chronic hepatitis C infection[10] in the development of IR. Because steatosis results in the overproduction of reactive oxygen species (ROS),[11] and ROS may exacerbate hepatic insulin sensitivity,[12] we hypothesized a close relationship between IR and oxidative stress. Therefore, we retrospectively analyzed the index of IR[13] and the serum and hepatic levels of thioredoxin (Trx), which are markers of oxidative stress,[14] in 203 patients with HCV infection. We also investigated whether relieving hepatic oxidative stress could improve IR among these patients.

METHODS

Patients

CHRONIC HEPATITIS PATIENTS who underwent liver biopsies in our institute between April 2003 and March 2006 were selected according to the following criteria: no excessive alcohol intake (more than 40 g/week), as assessed by interview (at least on 3 occasions); positive serum HCV-RNA, as confirmed by reverse transcription–polymerase chain reaction (RT–PCR); infection with HCV genotype 1 (1a, 1b) or 2 (2a, 2b); no history of antiviral therapy nor treatment with steatosis-inducing drugs within the 12 months before the study; negativity for hepatitis B surface antigen or antibodies to HIV; and an absence of other forms of chronic liver disease. Anthropometry and laboratory data were collected from all patients at the time of the liver biopsy. The serum HCV-RNA level was determined using the AMPLICOR GT HCV Monitor (Roche Diagnostic Systems, Tokyo, Japan). HCV genotypes 1 and 2 were determined by a serologic genotyping assay.[15] Serogroups 1 and 2 in this assay correspond to genotypes 1 (1a, 1b) and 2 (2a, 2b). Informed written consent was obtained from each patient. The study protocol conformed to the ethical guidelines of the 1975 Declaration of Helsinki approved by the Ethics Committee of the Kyoto Prefectural University of Medicine.

Laboratory determination

After a 12-h overnight fast, venous blood samples were drawn to determine alanine aminotransferase (ALT), γ-glutamylcysteine transpeptidases, fasting plasma glucose (FPG), insulin (IRI), triglyceride, and ferritin levels. These parameters were measured using standard techniques from clinical chemistry laboratories. The index of IR was calculated only in patients without overt diabetes (FPG >126 mg/dL), according to the homeostasis model assessment (HOMA).[13] The formula for IR was as follows: HOMA-IR = FPG (mg/dL) × IRI (μU/mL)/405. HOMA-IR was only calculated in patients without diabetes ($n = 189$).

Measurement of Trx

The levels of serum Trx were used as a marker of hepatic oxidative stress, as reported previously.[14] For the measurements of Trx concentrations, serum and liver biopsy specimens were stored at −80°C until use. The serum Trx levels were then measured using a commercial, sensitive enzyme-linked immunosorbent assay kit (REDOX BIOSCIENCE, Kyoto, Japan), as described previously.[14] All measurements were made in duplicate and average values were used for the statistical analysis.

The hepatic levels of Trx were measured by real-time PCR. Total RNA was isolated from biopsy specimens using the RNeasy kit (Qiagen, Hilden, Germany). The PCR mixture contained first-strand cDNA and specific primers for human Trx: sense, 5′-CTGCTTTTCAG GAAGCCTTG-3′ and antisense, 5′-ACCCACCTTTTGT CCCTTCT-3′. PCR was performed using the Light Cycler 2.0 System (Roche, Mannheim, Germany), and the mRNA levels of Trx were normalized to those of β-actin.

Histological evaluation

Formalin-fixed and paraffin-embedded liver biopsy specimens were stained with hematoxylin–eosin, Masson's trichrome, and Perl's Prussian blue. Degrees of hepatic fibrosis (stage) were scored as follows: F0 = none, F1 = portal expansion, F2 = bridging fibrosis, F3 = bridging fibrosis with lobular distortion, and F4 = cirrhosis. Degrees of inflammation (grade) were scored as follows: A0 = none, A1 = mild, A2 = moderate, and A3 = severe. Steatosis was assessed according to the percentage of hepatocytes containing fat droplets. The degree of iron loading was graded using a Perl's score of 0–4, as described previously.[16]

Phlebotomy

Phlebotomy was initiated to relieve iron-induced oxidative stress in 23 patients. All patients showed elevated serum ferritin levels and/or persistent abnormal ALT levels, and none showed anemia (hemoglobin <11.0 g/dL). They underwent phlebotomy (300–400 mL) either biweekly or monthly until serum ferritin levels were <20 ng/mL. Thereafter, the serum Trx levels and HOMA-IR were compared with baseline values in each

individual. However, treatments were terminated irrespective of serum ferritin levels when blood hemoglobin concentrations decreased to less than 10 g/dL.

Statistical analysis

The relationships between variables were analyzed using the Spearman's correlation coefficient by rank, and a partial correlation coefficient was calculated to remove the influence of confounding variables. Values after phlebotomy were compared with baseline values using a Wilcoxon rank sum test. All analyses were performed using SPSS software for Windows, version 14.0 (SPSS, Chicago, IL, USA). A *P*-value of less than 0.05 was considered significant.

RESULTS

General characteristics of and histological findings in patients

OF THE 309 HCV-infected patients who underwent liver biopsies, 203 patients met the criteria. Because many excessive drinkers among the male patients were excluded from the analysis, the number of females exceeded that of males in the study population. A summary of the clinical data for the liver biopsy findings in these patients is shown in Tables 1 and 2. Of the 203 patients that qualified, body mass index (BMI) was greater than 25 (kg/m^2) in 57 patients (28%), and 124 patients (61%) had a varying degree of hepatic steatosis, as shown in Table 2. Iron staining was performed in only 198 patients; a varying degree of iron loading was observed in 71 patients. Fourteen patients (7%) suffered from type 2 diabetes mellitus. The fibrosis scores of these patients were F1 in two patients, F2 in six, F3 in five, and F4 in only one. Seventy patients had received IFN-based antiviral therapy before the study and this treatment had failed to eradicate HCV.

Table 1 Baseline characteristics of patients

	Mean values of clinical data
Age	56.0 ± 11.9
Male/Female	73/146
BMI (kg/m^2)	22.9 ± 3.1
IFN: yes/no	70/133
ALT (IU/L)	75.5 ± 59.3
γ-GTP (U/L)	56.0 ± 51.0
FPG (mg/dl)	96.8 ± 13.1
HOMA-IR	2.3 ± 1.4
Ferritin (ng/ml)	174.2 ± 161.0
TG (mg/dl)	99.5 ± 50.5
Plt (×10^4/ml)	17.4 ± 5.3
HCV-RNA (KIU/ml)	1516 ± 1484.7
Serogroup 1/2	162/41
Trx (ng/ml)	30.4 ± 15.4

Data are expressed as mean ± standard deviation.
ALT, alanine aminotransferase; BMI, body mass index; FPG, fasting plasma glucose; γ-GTP, γ-glutamylcysteine transpeptidases; HCV, hepatitis C virus; HOMA-IR, homeostasis model assessment-insulin resistance; IFN, interferon; Plt, platelet; TG, triglyceride; Trx, thioredoxin.

Table 2 Histological findings on liver biopsy

	No. patients
F0/F1/F2/F3/F4	3/72/71/51/6
A0/A1/A2/A3	2/79/89/33
Steatosis:	
None	79
<10%	54
<30%	53
<60%	17
Iron load:	
Grade 0/1/2/3	127/33/25/13

Data are expressed as number of patients.

Predictors of the fibrosis score

The stage was significantly correlated with age, BMI, grade, grades of steatosis, iron score, ALT levels, platelet counts, ferritin levels, HOMA-IR, and serum Trx levels (Table 3). In a multiple regression analysis, grade, HOMA-IR, and serum Trx levels were shown to be

Table 3 Variables correlated with fibrosis scores

	Coefficient	Univariate	Multivariate
Age	$r = 0.163$	$P = 0.019$	$P = 0.931$
BMI	$r = 0.199$	$P = 0.004$	$P = 0.920$
Grade	$r = 0.869$	$P < 0.00001$	$P < 0.00001$
Steatosis	$r = 0.412$	$P < 0.00001$	$P = 0.761$
Iron score	$r = 0.155$	$P = 0.030$	$P = 0.437$
ALT	$r = 0.416$	$P < 0.00001$	$P = 0.259$
Plt	$r = -0.376$	$P < 0.00001$	$P = 0.119$
Ferritin	$r = 0.189$	$P = 0.010$	$P = 0.227$
HOMA-IR	$r = 0.406$	$P < 0.00001$	$P = 0.043$
Trx	$r = 0.365$	$P = 0.00006$	$P = 0.003$

Multiple regression analysis was used to analyze variables independently correlated with fibrosis scores.
ALT, alanine aminotransferase; BMI, body mass index; HOMA-IR, homeostasis model assessment-insulin resistance; Plt, platelet; Trx, thioredoxin.

independently correlated with stage (Table 3). Although the grade of steatosis is reported to predict rapid fibrosis progression,[5] it was not an independent variable in the multivariate analysis. Considering that IR is a major cause of hepatic steatosis,[11] HOMA-IR should be more significant than steatosis in this model.

Relationship between grades of steatosis and HOMA-IR or serum Trx levels

Steatosis has been considered to independently contribute to the progression of fibrosis in patients with chronic hepatitis C.[5] Therefore, we focused on the relationships between steatosis and either IR or oxidative stress. We found that grades of steatosis were significantly correlated not only with HOMA-IR, but also with serum Trx levels (HOMA-IR; $r = 0.344$, $P = 0.00002$: Trx; $r = 0.3$, $P < 0.001$). These findings suggested that oxidative stress could have a significant role in fibrosis progression through steatogenesis. We then focused on the relationship between IR and oxidative stress.

Relationship between HOMA-IR and serum Trx levels

HOMA-IR was significantly correlated with serum Trx levels (Fig. 1a: $r = 0.262$, $P = 0.012$) and BMI (Fig. 1b: $r = 0.302$, $P = 0.0002$). After adjustment for the effect of each variable using a corrected correlation coefficient, a significant relationship with HOMA-IR still remained for both serum Trx levels ($r = 0.244$, $P = 0.02$) and BMI ($r = 0.284$, $P = 0.006$). These results indicated that IR was attributable to oxidative stress, irrespective of obesity.

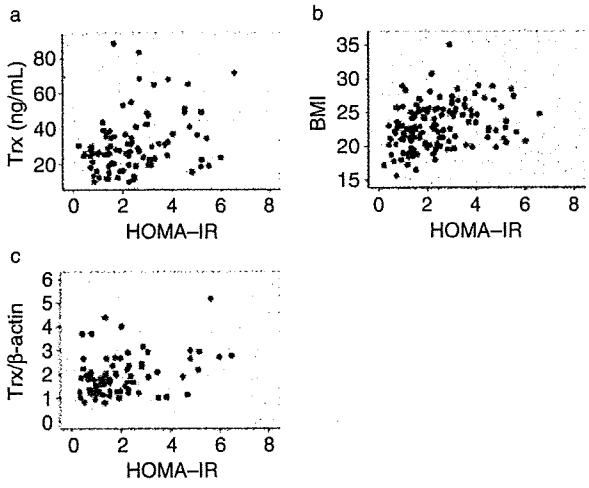

Figure 1 Correlation between homeostasis model assessment-insulin resistance (HOMA-IR) and serum levels of thioredoxin (Trx) (a), body mass index (BMI) (b), and mRNA levels of Trx (c). Both serum Trx levels and BMI were significantly correlated with HOMA-IR (serum Trx levels; $r = 0.262$, $P = 0.012$: BMI; $r = 0.302$, $P = 0.0002$). HOMA-IR was also significantly correlated with hepatic Trx levels ($r = 0.273$, $P = 0.014$).

Table 4 Factors correlated with HOMA-IR in subgroup patients ($n = 101$)

	Coefficient	Univariate	Multivariate
Hepatic Trx	$r = 0.273$	$P = 0.014$	$P = 0.011$
Grade	$r = 0.233$	$P = 0.038$	$P = 0.170$
Steatosis	$r = 0.286$	$P = 0.010$	$P = 0.251$
ALT	$r = 0.287$	$r = 0.010$	$r = 0.517$

Multiple regression analysis was used to analyze variables independently correlated with HOMA-IR.
ALT, alanine aminotransferase; HOMA-IR, homeostasis model assessment-insulin resistance; Trx, thioredoxin.

Relationship between HOMA-IR and hepatic Trx levels

Since Trx is known to be ubiquitously expressed,[17] we compared the mRNA levels of hepatic Trx with HOMA-IR in 101 patients whose liver biopsy specimens were available. The mRNA levels of Trx were significantly correlated with HOMA-IR (Fig. 1c: $r = 0.273$, $P = 0.014$). Among these patients, HOMA-IR also significantly correlated with grade, steatosis, and ALT levels (Table 4). In a multiple regression analysis, only the level of hepatic Trx was independently correlated with HOMA-IR (Table 4).

Effects of phlebotomy on ALT and serum Trx levels and HOMA-IR

All patients completed treatment without a significant change in body weight (age; 60.8 ± 10.8 kg, male/female; 15/8, BMI; 25.3 ± 2.6 kg/m^2, F0/F1/F2/F3/F4; 3/8/8/4, serogroup 1/2; 20/3). Nine patients had experienced IFN therapy before phlebotomy, whereas 14 patients had not experienced IFN therapy because of either old age or personal reasons. Changes in the serum levels of ALT, Trx, ferritin, HOMA-IR in the 23 patients that received phlebotomy are summarized in Table 5. Overall, the serum levels of ALT, Trx, and HOMA-IR were significantly decreased after phlebotomy compared with baseline values ($P < 0.00001$, $P = 0.023$, $P = 0.022$, respectively). These results indicated the efficacy of phlebotomy on insulin sensitivity as well as on liver function

Table 5 Changes in ALT, Trx, ferritin, and HOMA-IR after phlebotomy ($n = 23$)

	Before	After	Difference
BMI (kg/m^2)	23.6 (19.1–29.4)	24.0 (19.1–29.4)	NS
AST (IU/L)	67.0 (21–527)	51.0 (32–129)	$P < 0.005$
ALT (IU/L)	42.5 (27–121)	29.5 (24–53)	$P < 0.00001$
γ-GTP (IU/L)	89.0 (29–287)	60.5 (23–218)	$P < 0.0005$
Trx (ng/ml)	36.1 (20.2–79.4)	26.7 (18.1–32.7)	$P = 0.023$
Ferritin (ng/ml)	409.5 (125–1028)	20 (20–53)	$P < 0.00001$
HOMA-IR	3.5 (0.9–4.6)	2.4 (0.8–3.7)	$P = 0.022$

Data are expressed as medians (±range), Wilcoxon signed-ranks test.
ALT, alanine aminotransferase; AST, aspartate aminotransferase; BMI, body mass index; γ-GTP, glutamylcysteine transpeptidases; HOMA-IR, homeostasis model assessment–insulin resistance; Trx, thioredoxin.

tests in chronic hepatitis C patients. Furthermore, we analyzed the effects of phlebotomy on HOMA-IR in patients with a history of past IFN therapy and found that there were significant decreases in HOMA-IR (from 4.2 [3.7–4.6] to 2.9 [2.3–3.7], $P = 0.043$).

DISCUSSION

THE PRESENT STUDY shows that oxidative stress is an independent factor in the development of IR in patients with chronic hepatitis C, and validates the beneficial effect of phlebotomy on insulin sensitivity. To our knowledge, our report is the first to show a direct relationship between IR and oxidative stress in patients with HCV. We excluded alcohol drinkers, patients treated with steatosis-inducing drugs, and patients infected with HCV genotype 3a[18] from our analysis, as these are confounding factors affecting steatosis.

In general, the development of IR and steatosis is due to host-associated factors (e.g. obesity). The molecular mechanism underlying IR involves dysregulation of insulin-stimulated tyrosine phosphorylation of insulin receptor substrates (IRS).[19] This is achieved by phosphorylation of serine/threonine residues in IRS by either increased or decreased levels of adipokines associated with obesity (such as tumor necrosis factor [TNF]-α and adiponectin), thereby inhibiting tyrosine phosphorylation.[19] However, a high prevalence (61%) of steatosis, despite a low prevalence (28%) of obesity (BMI >25 kg/m^2) or diabetes (7%), indicated that there are mechanisms regulating insulin sensitivity other than obesity. In our study, HOMA-IR was significantly correlated with serum Trx levels, independent of BMI. Furthermore, the hepatic Trx levels independently predicted HOMA-IR in subgroup patients. Thus, hepatic oxidative stress directly contributes to IR in chronic hepatitis C patients.

Our hypothesis is supported by the following findings. First, chronic hepatitis C is characterized by oxidative stress-induced liver injury.[10,14,20] The overproduction of ROS could result from inflammatory cells,[10] iron overload,[20] and presumably the direct association of HCV core protein with mitochondria in hepatocytes.[21] In addition, steatosis, a prominent feature of chronic hepatitis C,[2–5] could result in oxidative stress.[11] Second, the increased abundance of ROS inhibits tyrosine phosphorylation of IRS in hepatocytes via the activation of stress-sensitive pathways, such as the c-Jun N-terminal kinase (JNK)[12] and nuclear factor (NF)-κB[22] pathways. JNK directly phosphorylates serine/threonine residues in IRS,[12] while NF-κB inhibits tyrosine phosphorylation via the induction of TNF-α.[22] The failure of hepatic insulin signaling subsequently leads to systemic IR.[12]

The question arising from this correlation between IR and oxidative stress is how metabolic disorders and liver injury can develop simultaneously in patients with HCV infection. One possible mechanism could be an interaction between IR and oxidative stress. IR results in hepatic steatosis,[11] which leads to increased ROS production concomitant with an increase in the number of inflammatory cells[10] and/or iron overload.[23] Conversely, ROS could exacerbate insulin sensitivity to promote steatosis,[11,12] and could promote the recruitment of inflammatory cells and fibrosis through lipid peroxidation products.[24,25] Thus, IR, steatosis, and oxidative stress could be involved in a feedback loop that exacerbates liver injury. This hypothesis is supported by the findings that HOMA-IR was significantly correlated with the serum and hepatic Trx levels, and both the HOMA-IR and serum Trx levels were significantly correlated with grades of steatosis.

Finally, we employed phlebotomy to validate the interaction between IR and oxidative stress, because

phlebotomy is useful for reducing hepatic oxidative stress.[20] Although phlebotomy is known to improve liver function tests in patients with HCV infection, its efficacy on insulin metabolism has not been well documented. Therefore, our findings provide new insight into the efficacy of phlebotomy. Notably, phlebotomy significantly improved HOMA-IR, even in patients who had been refractory to IFN. However, the long-term outcome of phlebotomy was unclear in this study, and a follow-up study should be performed.

In conclusion, we demonstrated an association between oxidative stress and IR in patients infected with HCV genotype 1 or 2. Our findings will contribute to our understanding of how metabolic disorders can develop in patients with chronic hepatitis C. Antioxidative therapy is a promising treatment to improve the pathogenesis of HCV.

REFERENCES

1 Dienstag JL, McHutchison JG. American gastroenterological association technical review on the management of hepatitis C. *Gastroenterology* 2006; **130**: 231–64.
2 Weinman SA, Belalcazar LM, Hepatitis C. a metabolic liver disease. *Gastroenterology* 2004; **126**: 917–19.
3 Monto A, Alonzo J, Watson JJ, Grunfeld C, Wright TL. Steatosis in chronic hepatitis C: relative contributions of obesity, diabetes mellitus, and alcohol. *Hepatology* 2002; **36**: 729–36.
4 Lonardo A, Adinolfi LE, Loria P, Carulli N, Ruggiero G, Day CP. Steatosis and hepatitis C virus: mechanisms and significance for hepatic and extrahepatic disease. *Gastroenterology* 2004; **126**: 586–97.
5 Adinolfi LE, Gambardella M, Andreana A, Tripodi MF, Utili R, Ruggiero G. Steatosis accelerates the progression of liver damage of chronic hepatitis C patients and correlates with specific HCV genotype and visceral obesity. *Hepatology* 2001; **33**: 1358–64.
6 El-Serag HB, Tran T, Everhart JE. Diabetes increases the risk of chronic liver disease and hepatocellular carcinoma. *Gastroenterology* 2004; **126**: 460–8.
7 DeFronzo RA, Ferrannini E. Insulin resistance. A multifaceted syndrome responsible for NIDDM, obesity, hypertension, dyslipidemia, and atherosclerotic cardiovascular disease. *Diabetes Care* 1991; **14**: 173–94.
8 Zekry A, McHutchison JG, Diehl AM. Insulin resistance and steatosis in hepatitis C virus infection. *Gut* 2005; **54**: 903–6.
9 Angulo P, Keach JC, Batts KP, Lindor KD. Independent predictors of liver fibrosis in patients with nonalcoholic steatohepatitis. *Hepatology* 1999; **30**: 1356–62.
10 Choi J, Ou JH. Mechanisms of liver injury III. Oxidative stress in the pathogenesis of hepatitis C virus. *Am J Physiol Gastrointest Liver Physiol* 2006; **290**: 847–51.
11 Browning JD, Horton JD. Molecular mediators of hepatic steatosis and liver injury. *J Clin Invest* 2004; **114**: 147–52.
12 Evans JL, Goldfine ID, Maddux BA, Grodsky GM. Are oxidative stress-activated signaling pathways mediators of insulin resistance and beta-cell dysfunction? *Diabetes* 2003; **52**: 1–8.
13 Matthews DR, Hosker JP, Rudenski AS, Naylor BA, Treacher DF, Turner RC. Homeostasis model assessment: insulin resistance and beta-cell function from fasting plasma glucose and insulin concentrations in man. *Diabetologia* 1985; **28**: 412–19.
14 Sumida Y, Nakashima T, Yoh T *et al.* Serum thioredoxin levels as an indicator of oxidative stress in patients with hepatitis C virus infection. *J Hepatol* 2000; **33**: 616–22.
15 Tsukiyama-Kohara K, Yamaguchi K, Maki N *et al.* Antigenicities of group I and II hepatitis C virus polypeptides – molecular basis of diagnosis. *Virology* 1993; **192**: 430–7.
16 Searle JW, Kerr JFR, Halliday JW, Powell LW. *Pathology of the Liver*, 2nd edn. Edinburgh: Churchill Livingstone, 1987.
17 Kondo N, Nakamura H, Masutani H, Yodoi J. Redox regulation of human thioredoxin network. *Antioxid Redox Signal* 2006; **8**: 1881–90.
18 Castera L, Hezode C, Roudot-Thoraval F *et al.* Effect of antiviral treatment on evolution of liver steatosis in patients with chronic hepatitis C: indirect evidence of a role of hepatitis C virus genotype 3 in steatosis. *Gut* 2004; **53**: 420–4.
19 Birnbaum MJ. Turning down insulin signaling. *J Clin Invest* 2001; **108**: 655–9.
20 Kato J, Kobune M, Nakamura T *et al.* Normalization of elevated hepatic 8-hydroxy-2'-deoxyguanosine levels in chronic hepatitis C patients by phlebotomy and low iron diet. *Cancer Res* 2001; **61**: 8697–702.
21 Korenaga M, Wang T, Li Y *et al.* Hepatitis C virus core protein inhibits mitochondrial electron transport and increases reactive oxygen species (ROS) production. *J Biol Chem* 2005; **280**: 37481–8.
22 Day CP. From fat to inflammation. *Gastroenterology* 2006; **130**: 207–10.
23 Liu D, Liu J, Wen J. Elevation of hydrogen peroxide after spinal cable injury detected by using the Fenton reaction. *Free Radic Biol Med* 1999; **27**: 478–82.
24 Esterbauer H, Schaur RJ, Zollner H. Chemistry and biochemistry of 4-hydroxynonenal, malonaldehyde and related aldehydes. *Free Radic Biol Med* 1991; **11**: 81–128.
25 Parola M, Robino G. Oxidative stress-related molecules and liver fibrosis. *J Hepatol* 2001; **35**: 297–306.

Association of Gankyrin Protein Expression with Early Clinical Stages and Insulin-Like Growth Factor-Binding Protein 5 Expression in Human Hepatocellular Carcinoma

Atsushi Umemura,[1,2] Yoshito Itoh,[2] Katsuhiko Itoh,[1] Kanji Yamaguchi,[2] Tomoki Nakajima,[2] Hiroaki Higashitsuji,[1] Hitoshi Onoue,[3] Manabu Fukumoto,[4] Takeshi Okanoue,[2] and Jun Fujita[1]

Gankyrin (also known as PSMD10) is a liver oncoprotein that interacts with multiple proteins including MDM2 and accelerates degradation of the tumor suppressors p53 and Rb. We produced a monoclonal anti-gankyrin antibody and immunohistochemically assessed the clinicopathological significance of gankyrin overexpression in 43 specimens of human hepatocellular carcinoma (HCC). Specific cytoplasmic staining for gankyrin was observed in 62.8% (27/43) of HCCs, which was significantly associated with low TNM stage ($P = 0.004$), no capsular invasion ($P = 0.018$), no portal venous invasion ($P = 0.008$), and no intrahepatic metastasis ($P = 0.012$). The cumulative survival rate of patients with gankyrin-positive HCC was significantly higher than that with gankyrin-negative HCC ($P = 0.037$). p53 and MDM2 were positively stained by antibodies in 30.2% and 23.3%, respectively, of HCCs, but neither was inversely associated with gankyrin expression. In the Huh-7 human HCC cell line, overexpression of gankyrin up-regulated expression of insulin-like growth factor binding protein 5 (IGFBP-5), whereas suppression of gankyrin expression by siRNA down-regulated it. Supression of IGFBP-5 expression inhibited proliferation of Huh-7 cells as well as U-2 OS osteosarcoma cells. In HCC specimens, positive staining for IGFBP-5 was observed by immunohistochemistry in 41.9% (18/43), and the level of expression was significantly correlated with that of gankyrin ($rho = 0.629$, $P < 0.001$). *Conclusion:* These results suggest that gankyrin plays an oncogenic role(s) mainly at the early stages of human hepatocarcinogenesis, and that IGFBP-5 inducible by gankyrin overexpression may be involved in it. (HEPATOLOGY 2008;47:493-502.)

Liver cancer is the sixth most common cancer worldwide (626,000 or 5.7% of new cancer cases) and the third most common cause of death from cancer (598,000) in 2002.[1] Eighty-two percent of cases are in developing countries, and the areas of high incidence are sub-Saharan Africa, eastern and southeastern Asia, and Melanesia. Histologically, more than 90% of the primary liver cancers are hepatocellular carcinomas (HCCs). Although there are several modalities of treatment for HCC, most patients present with unresectable tumors, and nonsurgical treatments are minimally effective at best.[2,3] Even for those patients who undergo surgical resection, the recurrence rate is very high and the prognosis is poor.[2,4-6] It is therefore important to clarify the mechanisms of human hepatocarcinogenesis and identify molecular targets to develop novel diagnostic, therapeutic, and preventive strategies.

By constructing subtracted complementary DNA (cDNA) libraries, we have previously identified 19 genes overexpressed in HCCs including 2 novel genes.[7,8] One of them was named gankyrin (gann-ankyrin repeat pro-

Abbreviations: 3A6C2, mouse monoclonal anti-gankyrin antibody; cDNA, complementary DNA; HCC, hepatocellular carcinoma; IGF, insulinlike growth factor; IGFBP-5, insulin-like growth factor-binding protein 5; MDM2, mouse double minute 2; mRNA, messenger RNA; RT-PCR, reverse transcription polymerase chain reaction; siRNA, short interfering RNA; TNM, tumor-node-metastasis.

From the [1]Department of Clinical Molecular Biology, Graduate School of Medicine, Kyoto University, Kyoto, Japan; the [2]Molecular Gastroenterology and Hepatology, Graduate School of Medical Science, Kyoto Prefectural University of Medicine, Kyoto, Japan; the [3]Department of Nutritional Science, Faculty of Health and Welfare, Seinan Jo Gakuin University, Kitakyushu, Japan; and the [4]Department of Pathology, Institute of Development, Aging, and Cancer, Tohoku University, Sendai, Japan

Received May 21, 2007; accepted September 3, 2007.

Supported by Grants-in aid from the Ministry of Education, Culture, Sports, Science, and Technology of Japan and the Japan Society for the Promotion of Science.

Address reprint requests to: Jun Fujita, Department of Clinical Molecular Biology, Graduate School of Medicine, Kyoto University, 54 Shogoin Kawaharacho, Sakyo-ku, Kyoto 606-8507, Japan. E-mail: jfujita@virus.kyoto-u.ac.jp; fax: (81) 75-751-4977.

Published online in Wiley InterScience (www.interscience.wiley.com).

DOI 10.1002/hep.22027

Potential conflict of interest: Nothing to report.

tein; "gann" in Japanese means cancer).[9] Gankyrin (also called PSMD10) consists of 7 ankyrin repeats, and its messenger RNA (mRNA) was overexpressed in 34 of 34 HCCs analyzed.[9,10] Independently, gankyrin was isolated as the p28 component or the interactor of the S6b subunit of the 19S regulator of the 26S proteasome.[11,12] The ankyrin repeat is the functional domain involved in protein–protein interactions, and gankyrin has been shown to interact with multiple proteins in addition to S6b. Gankyrin binds to retinoblastoma protein (Rb) and cyclin-dependent kinase (Cdk4), and accelerates phosphorylation and degradation of Rb, which results in release of the E2F transcription factor to activate DNA synthesis genes.[9,13] Gankyrin seems to play a role in cell cycle progression in noncancerous cells as well. Overexpression of gankyrin shortens population doubling time of NIH/3T3 mouse fibroblasts,[9] and its up-regulation correlates with cell cycle progression in normal rat primary hepatocytes, oval cells, and human hepatocytes.[14,15]

Overexpression of gankyrin confers tumorigenicity to NIH/3T3 cells and inhibits apoptosis in cultured human tumor cells exposed to chemotherapeutic agents.[10] The anti-apoptotic activity is attributable, at least partly, to increased degradation of p53, resulting in the reduced transcription of the p53-dependent proapoptotic genes.[16] Gankyrin binds to the E3 ubiquitin ligase MDM2 *in vitro* and *in vivo,* which increases p53–MDM2 association, thereby facilitating the ubiquitination and subsequent proteasomal degradation of p53 by MDM2. Gankyrin also controls MDM2 auto-ubiquitination and degradation, especially in the absence of p53.[16]

We produced a mouse monoclonal antibody against human gankyrin and assessed the expression of gankyrin protein in surgically resected HCC specimens by immunohistochemistry. Correlation of gankyrin positivity with clinicopathological findings and expression of p53 and MDM2 in HCC was analyzed. Furthermore, we demonstrated that expression of insulin-like growth factor-binding protein 5 (IGFBP-5) is inducible by overexpression of gankyrin in HCCs.

Patients and Methods

Patients and Specimens. HCC tissues and their corresponding noncancerous liver tissues were obtained from 43 and 32 patients, respectively, who had undergone curative hepatectomy at the University Hospital of Kyoto Prefectural University of Medicine between 1992 and 2000. The specimens used were routinely processed, formalin-fixed, and paraffin-embedded. After hematoxylin-eosin staining, all samples were diagnosed as HCC and the tumor-node-metastasis (TNM) classification was made according to the fourth edition of the general rules for the clinical and pathological study of primary liver cancer proposed by the Liver Cancer Study Group of Japan.[17] The demographic profiles of the patients are summarized in Table 1. For western blot analysis, HCCs and noncancerous liver tissues were obtained from 3 patients undergoing liver transplantation at the University Hospital of Kyoto Prefectural University of Medicine between 2004 and 2006. No donor organs were obtained from executed prisoners or other institutionalized persons. The study protocol conformed to the ethical guidelines of the 1975 Declaration of Helsinki and was approved by the institutional review boards. Written informed consents were obtained from all patients for subsequent use of their resected tissues.

Table 1. Patient and Tumor Characteristics

Characteristic	Number (Percentage)
Number of patients	43
Sex distribution	
Male	27 (62.8%)
Female	16 (37.2%)
Age (years)	25-78, median 65
Virus marker	
HBV(+)/HCV(−)	6 (14.0%)
HBV(−)/HCV(+)	28 (65.0%)
HBV(+)/HCV(+)	3 (7.0%)
HBV(−)/HCV(−)	6 (14.0%)
AFP(ng/mL)	3.5-39999, median 90
Tumor size (cm)	1.6-17.0, median 4.0
Liver cirrhosis	
Yes	29 (67.5%)
No	14 (32.5%)
Chronic hepatitis	13 (30.2%)
Normal	1 (2.3%)
TNM stage	
I	4 (9.3%)
II	22 (51.1%)
III	8 (18.6%)
IV	9 (21.0%)
Histological differentiation	
Well	12 (27.9%)
Moderate	25 (58.1%)
Poor	6 (14.0%)
Capsular formation	
Yes	36 (83.7%)
No	7 (16.3%)
Capsular invasion	
Yes	14 (32.6%)
No	29 (67.4%)
Portal venous invasion	
Yes	9 (20.9%)
No	34 (79.1%)
Intrahepatic metastasis	
Yes	16 (37.2%)
No	27 (62.8%)

Abbreviations: HCV(+), anti-hepatitis C virus antibody positive; HBV(+), hepatitis B surface antigen positive; (−), negative; AFP, serum alpha-fetoprotein.

Cell Culture and Transfection. Huh-7 human HCC cells, U-2 OS human osteosarcoma cells, 293T human embryonic kidney cells, mouse lymph node cells, and P3X63Ag8U.1 mouse myeloma cells were cultured in Dulbecco's modified Eagle's medium (Gibco BRL Life Technologies, NY) supplemented with 10% fetal bovine serum as described.[16] To assess viable cell numbers, we used the Dojindo Cell Counting Kit-8 (CCK8 kit, Dojindo Laboratories, Kumamoto, Japan) according to the manufacturer's instructions.

The 293T, Huh-7, and U-2 OS cells were transfected with plasmid DNA by using the calcium phosphate method or FuGENE 6 Transfection Reagent (Roche Diagnostics, Mannheim, Germany) as described.[16] Short interfering RNA (siRNA) were transfected at a final concentration of 25 nM by using siPORT NeoFX Transfection Agent (Ambion, Austin, TX) following the manufacturer's instructions. Twenty-four hours after transfection, the medium was replaced with fresh medium containing fetal bovine serum, and the culture was continued for another 24 or 48 hours. Then, the cells were harvested for analysis. All transfection assays were repeated at least 3 times.

Plasmids and siRNA. Human wild-type gankyrin cDNAs, full coding sequence and deletion mutants, were cloned into the mammalian expression vector pMKIT-NEO and expressed as hemagglutinin (HA)-tagged proteins (Fig. 1A). Full-length gankyrin was expressed without a tag as well. To obtain recombinant human gankyrin protein, the full-length cDNA was cloned into an expression vector derived from pET28 (Novagen, EMD Biosciences Inc., San Diego, CA) and expressed as hexahistidine-tagged protein.

To down-regulate gene expression, Silencer Predesigned siRNAs for gankyrin (Ambion) and Stealth Select iRNA: for IGFBP-5 (Invitrogen, Tokyo, Japan), were used together with respective control RNAs.

Antibodies. To obtain monoclonal antibodies against human gankyrin, recombinant (His)6-gankyrin protein was used as an immunogen. It was dissolved in phosphate-buffered saline (1 mg/mL) and emulsified with an equal volume of Freund's complete adjuvant (Difco, Becton-Dickinson, Franklin Lakes, NJ). Two female BALB/c mice were injected with the emulsion (50 μL/mouse) in the footpad. Two weeks after immunization, the inguinal lymph node cells (4×10^7 cells) were fused with P3X63Ag8U.1 myeloma cells (1×10^7) using polyethylene glycol 1500 (Roche Diagnostics). Fused cells were cultured in 96-well plates at 2×10^5 cell/well. The supernatants were assayed for the anti-gankyrin antibody titer by an enzyme-linked immunosorbent assay using recombinant His-tagged, glutathione-S-transferase (GST)-tagged, and nontagged gankyrin proteins. Selected relevant hybridomas were cloned by the limiting dilution method, and the isotypes of secreted monoclonal antibodies were determined by the IsoStrip kit (Roche Diagnostics) following the manufacturer's instructions. Finally, an IgG2b kappa monoclonal antibody that showed the highest affinity for gankyrin was obtained and named 3A6C2.

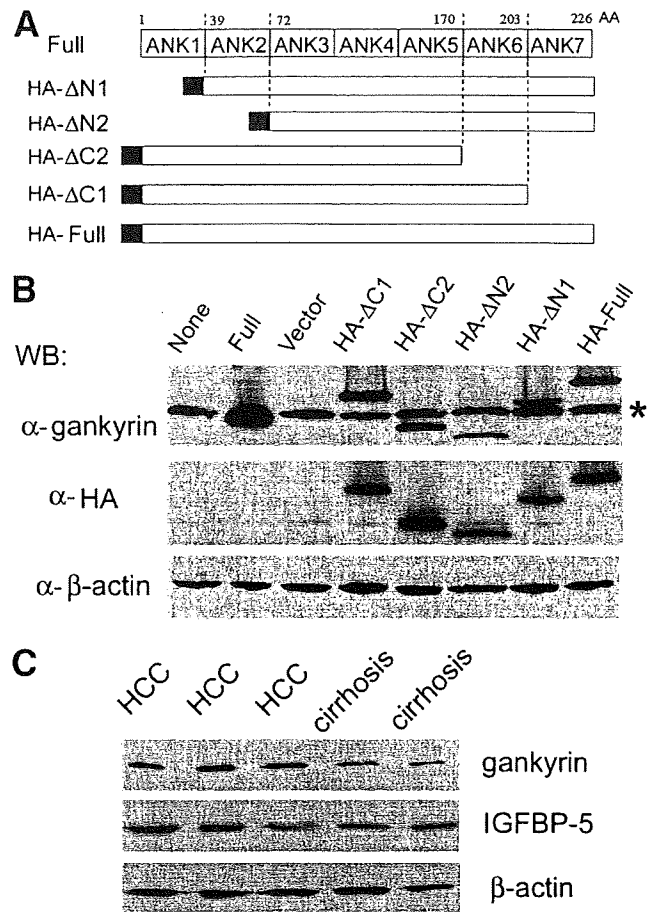

Fig. 1. Recognition of gankyrin protein by the monoclonal antibody. (A) Structures of wild-type gankyrin (Full) and its deletion mutants. Numbers on top, N- and C-terminal amino-acid residues. ANK, ankyrin repeat. Black bars, HA tags. (B) Specificity of the antibody. 293T cells were transfected with plasmids expressing the indicated proteins. Cell lysates were analyzed by western blotting (WB) using the anti-gankyrin monoclonal antibody (3A6C2), anti-HA antibody, and anti-β-actin antibody. *Mobility of the endogenous gankyrin. Representative results of 3 repeated experiments are shown. (C) Detection of gankyrin protein in tissues. Lysates were made from hepatocellular carcinoma (HCC, n = 3) and cirrhotic liver tissues (n = 2), and analyzed by WB using antibodies for indicated proteins. HA, hemagglutinin.

For western blot analysis, mouse monoclonal anti-gankyrin antibody (3A6C2), goat polyclonal anti–IGFBP-5 antibody (R&D Systems Inc., Minneapolis, MN), mouse monoclonal anti-HA antibody (12CA5, Roche Diagnostics), and mouse monoclonal anti–β-actin antibody (Chemicon International, Temecula, CA) were

used. Horseradish peroxidase–conjugated secondary antibodies against mouse or goat immunoglobulins were obtained from DAKO (Kyoto, Japan).

For immunohistochemistry, mouse monoclonal anti-gankyrin (3A6C2), anti-MDM2 (Ab-4, Oncogene research products, Boston, MA), and anti-p53 (DO-7, DAKO) antibodies, rabbit polyclonal anti-IGFBP-5 antibody (GroPep, Thebarton, Australia), and horseradish peroxidase–conjugated secondary antibodies against mouse or rabbit immunoglobulins (DAKO) were used.

Analysis of Gene Expression. Extraction of RNA, preparation of cell and tissue lysates, and western blot analysis were performed as described.[9] Real-time reverse transcription polymerase chain reaction (RT-PCR) analysis was performed using ABI PRISM 7900 (Applied Biosystems, Foster City, CA) and a 1-step QuantiTect RT-PCR Kit (Qiagen, Cowley, UK) according to the manufacturer's instructions. PCR conditions were 50°C for 30 minutes and 95°C for 15 minutes, followed by 45 cycles of 95°C for 15 seconds, 55°C for 30 seconds, and 72°C for 45 seconds. Specific PCR amplification products were detected by SYBR Green. Transcripts of β-actin were quantified as control. Primer sequences used were as follows: IGFBP-5, AAGAAGCTGACCCAGTCCAA and GAATCCTTTGCGGTCACAAT; gankyrin, GCAACTTGGAGTGCCAGTGAA and TCACTTGAGCACCTTTTCCCA; β-actin, CTACGTCGCCCTGGACTTCGAGC and GATGGAGCCGCCGATCCACACGG.

The immunohistochemical staining was performed on 4-μm-thick paraffin sections of tissues fixed in buffered formalin. The sections were pretreated with 10 mM citrate buffer (pH 6.1) in a microwave oven for 5 minutes. Endogenous peroxidase activity was blocked with 0.3 % H_2O_2 for 10 minutes. The sections were incubated with 10% fetal bovine serum for 30 minutes to reduce nonspecific binding, followed by incubation with the primary antibody at 4°C overnight. They were subsequently incubated with horseradish peroxidase–conjugated anti-mouse or rabbit immunoglobulin antibody for 30 minutes. The enzymatic reaction was developed in a freshly prepared solution of 3,3′-diaminobenzidine tetrahydrochloride using DAKO Liquid DAB Substrate-Chromogen Solution for 10 minutes at room temperature. The sections were then counterstained with hematoxylin. The staining pattern, the distribution of the immunostaining in each tissue, and the intensity of the staining were studied in detail. Negative controls were conducted by substituting normal sera of each animal for the primary antibodies. When immunoreactivities were heterogenously observed, cases with moderate or strong staining of nucleus or cytoplasm in more than 5% of the cells were considered positive. To analyze the correlation of the expression levels of gankyrin and IGFBP-5, the staining intensity was expressed as 0 (negative), 1+ (weakly positive), 2+ (moderately positive), or 3+ (strongly positive). In each case the immunoreactivity was determined in 5 random high-powered fields and the count was done independently by 2 observers.

Statistical Analysis. Categorical variables were compared using Fisher's exact test. Paired comparison of continuous data was performed using the Wilcoxon signed ranks test. To assess whether the 2 variables covary, Spearman's rank correlation coefficient was determined. Cumulative survival curves were calculated by the Kaplan-Meier method and analyzed by the log-rank test. All statistical analyses were performed using the JMP statistical software package (SAS Institute Inc., Cary, NC). A P value less than 0.05 was considered statistically significant.

Results

Clinicopathological Profiles. Forty-three patients with HCC were recruited in this study, including 27 men and 16 women, with ages ranging from 25 to 78 (median 65) years old. Clinicopathological profiles of the patients and their HCCs are shown in Table 1. Antibody to hepatitis C virus was found in sera of 72% of the patients, and hepatitis B virus surface antigen was positive in 21%.

According to the TNM staging, 60% were stage I to II and 40% were stage III to IV. In noncancerous portions of the resected livers, cirrhosis and chronic hepatitis[18] were found in 68% and 30%, respectively, of the specimens, whereas only 1 (2%) was of normal histology. Fibrocapsular formation surrounding HCC was observed in 84% and capsular invasion by HCC cells in 33%. Portal vein involvement and satellite nodules suggesting intrahepatic metastasis were found in 21% and 37%, respectively.

Detection of Gankyrin with the Monoclonal Anti-gankyrin Antibody. To determine the specificity of the monoclonal anti-gankyrin antibody 3A6C2, we expressed wild-type full-length or truncated gankyrin (Fig. 1A) in 293T cells. The antibody detected all mutants of gankyrin, suggesting that the epitope exists within the third and fifth ankyrin-repeat region (Fig. 1B). The antibody recognized the endogenous gankyrin as well, and no major cross-reacting band was observed.

Because gankyrin mRNA is known to be overexpressed in most HCCs,[9] we analyzed the levels of gankyrin protein in HCCs and surrounding noncancerous liver tissues using the 3A6C2 antibody. The protein level of gankyrin was higher in HCC tissues than in noncancerous tissues

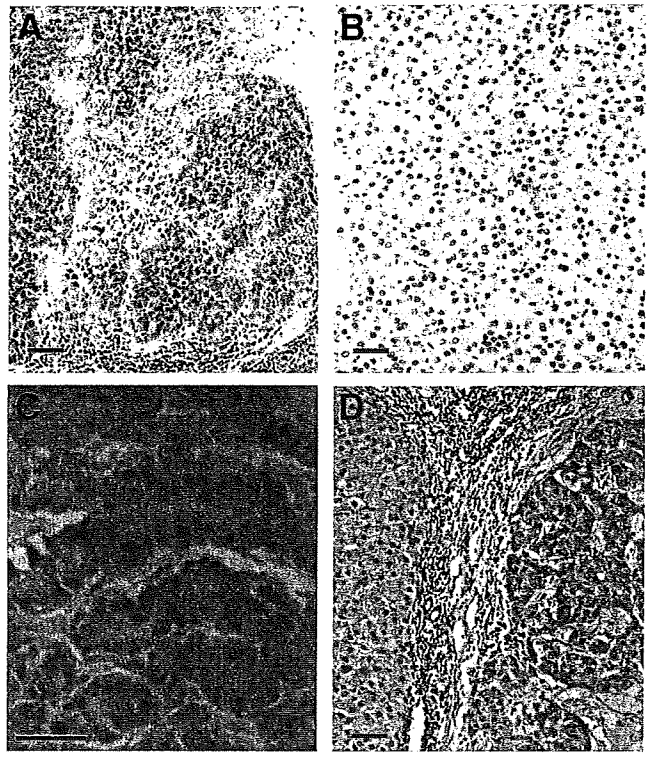

Fig. 2. Immunohistochemical detection of gankyrin in hepatocellular carcinoma (HCC). HCC sections were stained with mouse monoclonal anti-gankyrin antibody, and counterstained with hematoxylin. Positive immunostaining appears brown. (A) Positive staining for gankyrin in the cytoplasm of most HCC cells. (B) Barely detectable gankyrin signal in some HCC cells. (C) Presence of gankyrin in the nucleus of some HCC cells. (D) Stronger staining for gankyrin in HCC cells (right) than the neighboring cirrhotic hepatocytes (left). Bar, 50 μm.

(Fig. 1C). The mobilities of the gankyrin band were not different among samples.

Immunohistochemical Analysis of Gankyrin Expression. We next examined the expression of gankyrin protein in HCC and noncancerous liver tissues by immunohistochemistry. The gankyrin signal was observed mainly in the cytoplasm and occasionally in the nucleus of HCC cells (Fig. 2A-C). Although at lower levels compared with those in HCCs, weak but reproducible gankyrin signals were observed in the cytoplasm of the hepatocytes in the noncancerous tissues (Fig. 2D). Expression of gankyrin was not detected in the bile duct cells, blood endothelial cells, or other nonparenchymal cells in the liver tissues. Of 43 HCCs examined, the cytoplasm was stained positively for gankyrin in 27 (63%), and 9 of them (21%) were also positive for nuclear staining. Of 32 noncancerous liver tissues available, gankyrin was positive in 17 (53%).

As shown in Table 2, we analyzed an association between gankyrin protein expression and clinicopathological findings. No significant association between gankyrin expression in HCC cells and sex, age, tumor size, fibrotic change in noncancerous liver tissues, differentiation of the tumor cells, or hepatitis B or C virus infection was observed. Positive cytoplasmic staining for gankyrin of HCC cells was significantly associated with low TNM stage (stage I or II; $P = 0.004$), no capsular invasion ($P = 0.018$), no portal venous invasion ($P = 0.008$), and no intrahepatic metastasis ($P = 0.012$) of HCC. In noncancerous liver tissues, positive gankyrin staining of hepatocytes was associated with the cytoplasmic gankyrin positivity of HCC cells of the same patient ($P = 0.021$, Table 3), but not with the parameters examined except for the serum alpha-fetoprotein level ($P = 0.015$, Table 2).

Because expression of gankyrin affects the degradation of p53 and MDM2,[16] we examined the expression of p53 and MDM2 as well as gankyrin in HCCs. By immunohistochemistry, nuclear expression of p53 and MDM2 were detected in 30% and 23%, respectively, of 43 HCCs (Fig. 3, Table 3). Positive staining for gankyrin was not associated with the staining for p53 nor MDM2 in HCC cells.

Up-regulation of IGFBP-5 Expression by Gankyrin in HCCs. Preliminary microarray analysis of the cDNA libraries prepared from U-2 OS cells and Huh-7 cells overexpressing gankyrin suggested that IGFBP-5 mRNA was up-regulated by gankyrin (A. Umemura and J. Fujita, unpublished data). Real-time RT-PCR analysis con-

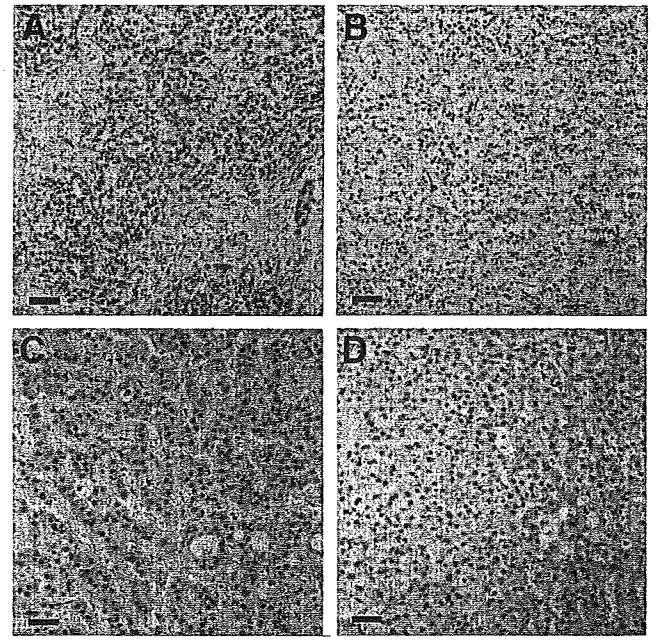

Fig. 3. Immunohistochemical detection of p53 and MDM2 in hepatocellular carcinoma (HCC). HCC sections were stained with antibodies specific to p53 (A and B) or MDM2 (C and D), and counterstained with hematoxylin. Positive immunostaining appears brown. (A) Positive staining for p53 in the nucleus of most HCC cells. (B) Negative p53 in HCC cells. (C) Positive staining for MDM2 in the nucleus of most HCC cells. (D) Negative MDM2 in HCC cells. Bar, 50 μm.

Table 2. Gankyrin Expression and Clinicopathological Characteristics

	Gankyrin Expression in the Cytoplasm of					
	HCC			Noncancerous Liver		
	Negative (n = 16)	Positive (n = 27)	*P* value	Negative (n = 15)	Positive (n = 17)	*P* value
Sex distribution						
Male	12	15	0.328	10	11	1.000
Female	4	12		5	6	
Median age (years)	64	65	0.696	63	62	0.649
Virus marker			NS			NS
HBV(+)/HCV(−)	3	3		2	2	
HBV(−)/HCV(+)	10	18		11	11	
HBV(+)/HCV(+)	1	2		2	0	
HBV(−)/HCV(−)	2	4		0	4	
Median AFP (ng/mL)	63.0	95.0	0.890	25.0	199.0	0.015
Median tumor size (cm)	4.5	4.0	0.098	4.5	4.0	0.372
Liver cirrhosis (+)	9	20	0.316	9	13	0.450
TNM stage						
I and II	5	21	0.004	8	12	0.467
III and IV	11	6		7	5	
Histological differentiation						
Well	5	7	0.737	6	3	0.243
Moderate and poor	11	20		9	14	
Capsular formation (+)	15	21	0.229	12	13	1.000
Capsular invasion (+)	9	5	0.018	4	6	0.712
Portal venous invasion (+)	7	2	0.008	4	3	0.678
Intrahepatic metastasis (+)	10	6	0.012	6	5	0.712
Gankyrin nuclear expression						
Yes	0	9	0.016	2	5	0.403
No	16	18		13	12	

Abbreviations: HCV, anti-hepatitis C virus antibody; HBV, hepatitis B surface antigen; (+), positive or present; (−), negative or absent; AFP, serum alpha-fetoprotein; NS, not significant between any groups or combinations thereof.

firmed that overexpression of gankyrin increased the IGFBP-5 mRNA levels 5.2-fold and 1.7-fold (mean, n = 3 each) in U-2 OS and Huh-7 cells, respectively, and western blot analysis demonstrated that the protein levels were increased as well (Fig. 4A). Conversely, when gankyrin expression was suppressed by siRNA, IGFBP-5 expression was down-regulated (Fig. 4B). In 2 of 3 HCC tissues overexpressing gankyrin, the levels of IGFBP-5 protein were higher compared with those in noncancerous tissues (Fig. 1C). To identify a role that IGFBP-5 might play in HCC cells, we next suppressed IGFBP-5 expression by siRNA. No apoptosis was induced, but viable cell numbers were decreased in Huh-7 as well as U-2 OS cells (Fig. 4C,D, and data not shown), suggesting a growth-promoting effect of IGFBP-5.

The expression of IGFBP-5 was further examined immunohistochemically in 43 HCC and 32 noncancerous liver tissues (Fig. 5, Table 3). In 42% of HCCs, IGFBP-5 was positively stained in the cytoplasm of HCC cells (Fig. 5A). IGFBP-5 was also detected, although at lower levels, in the cytoplasm of hepatocytes in 28% of the noncancerous tissues (Fig. 5B-D), but not in bile duct cells, blood endothelial cells, or other nonparenchymal cells.

Specific cytoplasmic staining for IGFBP-5 in HCC cells was associated with low TNM stage (stage I or II; $P = 0.013$), no portal venous invasion ($P = 0.006$), low serum alpha-fetoprotein value ($P = 0.031$), and small tumor size ($P = 0.009$). No association with capsular invasion or intrahepatic metastasis was observed. There was a significant association between positivities for IGFBP-5 and

Table 3. Gankyrin Expression and Molecular Histological Markers

	Gankyrin Expression in HCC		
	Negative	Positive	*P* value
Gankyrin expression in non-HCC			
Negative (n = 15)	8	7	0.021
Positive (n = 17)	2	15	
p53 expression in HCC			
Negative (n = 30)	11	19	1.000
Positive (n = 13)	5	8	
MDM2 expression in HCC			
Negative (n = 33)	14	19	0.276
Positive (n = 10)	2	8	
IGFBP-5 expression in HCC			
Negative (n = 25)	13	12	0.026
Positive (n = 18)	3	15	
IGFBP-5 expression in non-HCC			
Negative (n = 23)	14	9	0.011
Positive (n = 9)	1	8	

Abbreviations: HCC, hepatocellular carcinoma; non-HCC, noncancerous portion of the resected liver; IGFBP-5, insulin-like growth factor-binding protein 5.

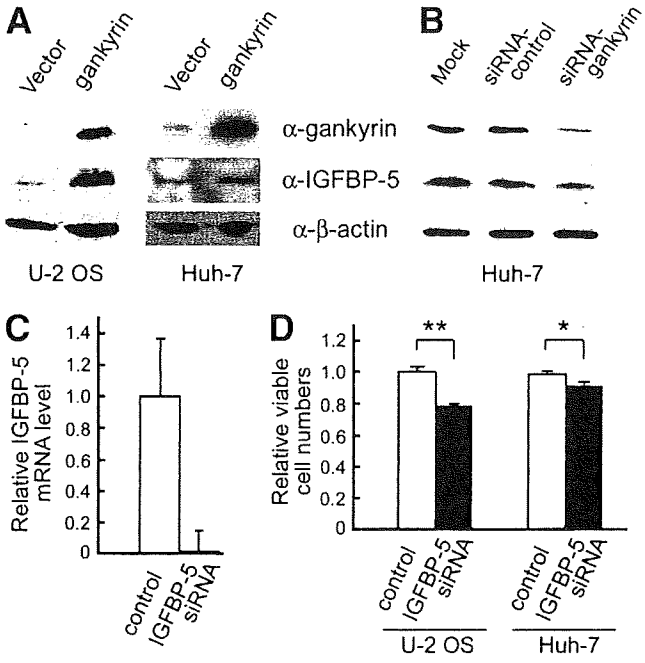

Fig. 4. Induction of IGFBP-5 by gankyrin. (A) U-2 OS cells (lanes 1 and 2) and Huh-7 cells (lanes 3 and 4) transiently transfected with plasmids expressing gankyrin or vector alone were analyzed for expression of IGFBP-5 by western blotting using the indicated antibodies. Representative results from more than 3 experiments are shown. (B) Huh-7 cells, mock transfected or transfected with siRNA for gankyrin or control RNA as indicated, were analyzed as in (A). (C) Suppression of IGFBP-5 expression by siRNA. Huh-7 cells were transfected with control RNA or IGFBP-5-specific siRNA. IGFBP-5 transcript levels were determined by real-time RT-PCR and normalized with β-actin levels. Results from 3 repeats were averaged and expressed relative to control. Error bars refer to standard deviation of the average quantitated results. (D) Effect of IGFBP-5 down-regulation on cell growth. U-2 OS and Huh-7 cells were transfected with IGFBP-5 siRNA or control RNA, and 72 hours later viable cell numbers were determined. Values are mean ± standard deviation (n = 3) and expressed relative to controls. ** and *, $P < 0.01$ and $P < 0.05$, respectively.

gankyrin (Table 3), and the levels of expression covaried both in HCCs ($\rho = 0.629$, $P < 0.001$) (Fig. 5E) and noncancerous hepatocytes ($\rho = 0.606$, $P < 0.001$) (Fig. 5F).

Expression of Gankyrin in HCC and Patient Prognosis. When we examined the relationship between gankyrin expression in HCC cells and the survival of patients after surgical resection, a significant difference was observed between the patients with gankyrin-positive HCCs and those with gankyrin-negative HCCs (Fig. 6). We found no significant difference in the survival rates between the patients whose HCCs stained positively and negatively for p53, MDM2, or IGFBP-5.

Discussion

Gankyrin is as an oncogene, mRNA of which is overexpressed in almost all human HCCs.[9,19] Although less frequent, gankyrin has been found by RNA dot blot analysis to be overexpressed in additional tumors including those of the breast, colon, rectum, stomach, small intestine, pancreas, ovary, lung, and thyroid (A. Umemura and J. Fujita, unpublished data). In the current study, we immunohistochemically examined the gankyrin protein expression in HCCs using the monoclonal anti-gankyrin antibody and found that the protein was highly expressed in the cytoplasm of 63% of HCCs. Tan et al.[20] has simi-

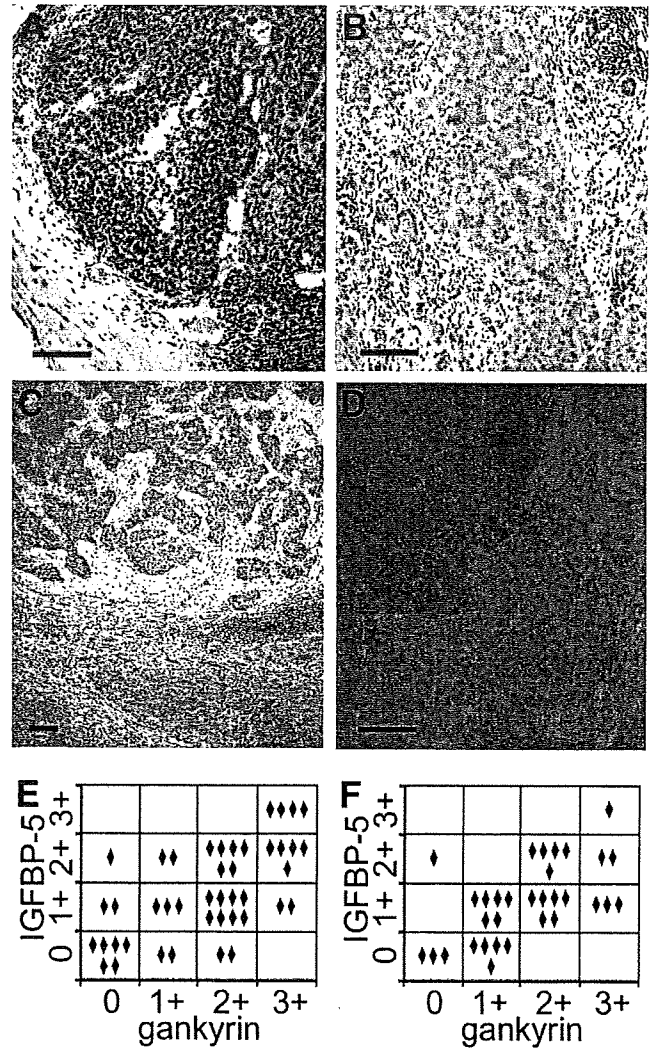

Fig. 5. Immunohistochemical detection of IGFBP-5 in hepatocellular carcinoma (HCC). HCC sections were stained with anti-IGFBP-5 antibody and counterstained with hematoxylin. Positive immunostaining appears brown. (A) Positive staining for IGFBP-5 in the cytoplasm of HCC cells, especially at the invasive boundaries. (B) Presence of IGFBP-5 in noncancerous cirrhotic hepatocytes. (C) Stronger staining for IGFBP-5 in HCC cells (upper) than the neighboring cirrhotic hepatocytes (lower). (D) Positive staining for IGFBP-5 in HCC cells (upper left), but negative in cirrhotic cells (lower right). Bar, 100 μm. (E) Correlation of expression levels of gankyrin and IGFBP-5 in HCCs. The immunostaining levels were expressed as 0 (negative), 1+ (weakly positive), 2+ (moderately positive), or 3+ (strongly positive). Each diamond represents 1 case. The Spearman's rho = 0.629, $P < 0.001$. (F) Correlation of expression levels of gankyrin and IGFBP-5 in noncancerous hepatocytes determined as in (E). The Spearman's rho = 0.606, $P < 0.001$.

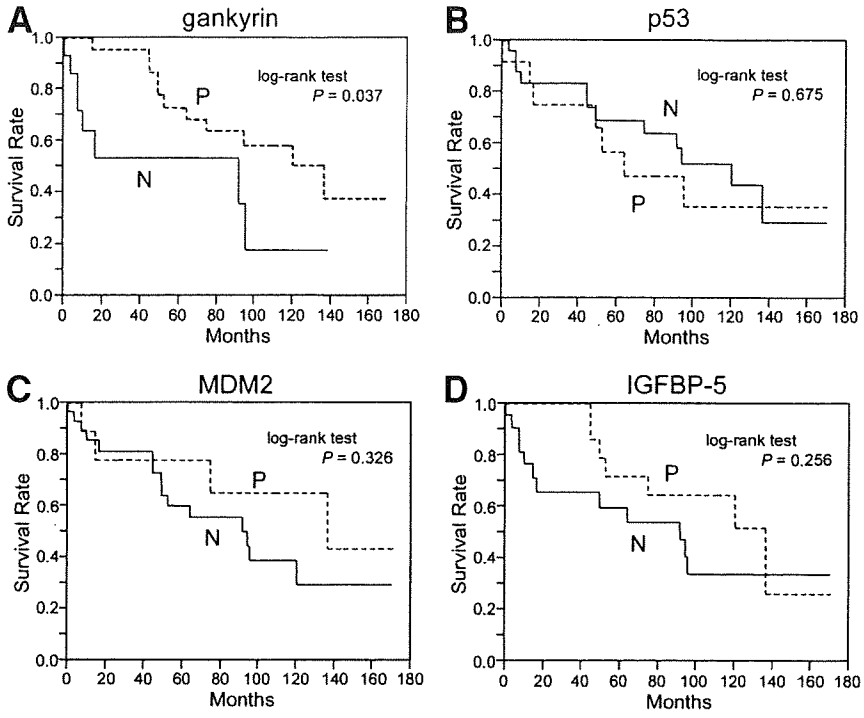

Fig. 6. Survival of patients and expression of molecular markers. The Kaplan-Meier method was used to determine the patient survival and log-rank test to compare survival between patients with HCC grouped according to (A) gankyrin positivity, (B) p53 positivity, (C) MDM2 positivity, and (D) IGFBP-5 positivity. P, positive. N, negative.

larly found overexpression of gankyrin protein in 60% of HCCs using a polyclonal antibody. The reason why the protein is not overexpressed in one-third of HCCs despite overexpression of its mRNA is unknown. The posttranscriptional, translational, and posttranslational regulations of gankyrin expression remain to be elucidated.

According to the 15th follow-up survey by the Liver Cancer Study group of Japan, the cumulative survival rates after surgical removal of HCC are 52.3% and 27.3% at 5 and 10 years, respectively, and better survival rates are associated with fewer numbers of tumors, lack of portal venous invasion, and early clinical stages.[4-6] Consistent with these observations, gankyrin positivity of HCC was associated with low TNM stage, lack of capsular invasion, portal venous invasion, and intrahepatic metastasis, and better prognosis of the patients. Patients with hyperdiploid acute lymphoblastic leukemia with more than 50 chromosomes, one of the 6 subtypes of pediatric acute lymphoblastic leukemia, have an excellent prognosis compared with other subtypes, and interestingly, overexpression of gankyrin is 1 of the diagnostic and subclassification markers for it.[21] Expression of gankyrin protein may be used as a marker for better prognosis of the patients with HCC as well.

The gankyrin oncoprotein plays a key role in regulation of cell cycle and apoptosis, at least in cultured cells, by inhibiting Rb and p53.[10] In a rodent hepatocarcinogenesis model, hypermethylation of the p16INK4A gene and p53 mutation appear at a late stage, whereas gankyrin is overexpressed from early after carcinogen treatment, preceding the loss of Rb protein and adenoma formation.[22] Clinically, p53 mutation is not so frequent in HCCs (15%-30%), especially in low-grade or low-stage HCCs.[23,24] Tan et al.[20] have immunohistochemically detected gankyrin overexpression in 82%, 63%, and 22% of Edmondson's grade I to II, III, and IV HCCs, respectively. We observed gankyrin positivity in 81% and 35% of low and high TNM stage HCCs, respectively. These results suggest that gankyrin plays an important role(s) at early stages of hepatocarcinogenesis by suppressing Rb, p53 and possibly other tumor suppressors. In advanced HCCs, by contrast, oncogenic mutations probably have accumulated in many genes including p53, and overexpression of gankyrin may not be so crucial as in early stage HCCs. This could explain the present association of gankyrin-negative HCCs with poorer prognosis and the finding that both cases of gankyrin-negative HCCs with gankyrin-positive noncancerous hepatocytes belonged to high TNM stages. This is, however, one of several possible explanations, and further work is necessary to clarify the exact reasons for the observed association.

By immunohistochemical staining, p53 has been detected in 20% to 30% of HCCs.[25, 26] Although strong immunohistochemical reactivity for p53 may not be an indicator of the presence of p53 gene mutations as initially suggested,[26] it has been associated in some studies with higher proliferative activity, lower differentiation of HCC cells, or poorer survival of patients. Endo et al.[27] immunohistochemically detected MDM2 in 28 of 107 (26%) HCCs, and the positive expression correlated with

the presence of p53 mutation and poorer prognosis, although it also correlated with smaller HCC size and the absence of vascular invasion. We immunohistochemically detected the expression of p53 and MDM2 in 30% and 23%, respectively, of HCCs, which is in accord with other studies, but no correlation was seen between expression and survival of the patients. Gankyrin accelerates degradation of Rb, p53, and MDM2 in cultured cells.[9,16] Although some correlation between expression of gankyrin and Rb has been suggested in HCC tissues,[20] we did not observe significant relationship between the gankyrin positivity and negative staining for p53 nor MDM2. The analysis of individual cells for protein expression, for example by double 2-color immunostaining, may have revealed the presence of some relationship. But most probably, our finding reflects complex interrelated mechanisms regulating the levels of these proteins and also suggests that the relevance of the effects of gankyrin on p53, MDM2, and Rb demonstrated in cultured cells to human hepatocarcinogenic process remains to be firmly established.

The 6 members of IGFBP family (IGFBP-1 through IGFBP-6) are important components of the insulin-like growth factor (IGF) axis, and regulate the activity of both IGF-I and IGF-II polypeptide growth factors.[28] IGF-I, IGF-II, and their receptors are expressed in a wide variety of cells, and the liver is the main source of circulating IGF-I. IGFBPs are also secreted by many cell types, and their expression is regulated in a cell-dependent and tissue-type–dependent manner. In the current study, we found up-regulation of IGFBP-5 mRNA and protein levels by overexpression of gankyrin in human osteosarcoma and HCC cell lines and consistently detected a significant association between the protein levels of gankyrin and IGFBP-5 in HCC specimens. In the proximal promoter region of the IGFBP-5 gene, there are several putative transcription-factor–binding sites including those for AP-2, c-Myb, C/EBP, and NF-1, and responsive elements to prostaglandin E_2, cyclic adenosine monophosphate, progesterone/retinoic acid, and Akt.[28] Whether the effect of gankyrin on IGFBP-5 expression is mediated by these factors is unknown.

The IGFBPs bind IGFs with high affinity, and they are able to enhance or inhibit the activity of IGFs in a cell-specific and tissue-type–specific manner.[28] In addition, IGFBPs have IGF-independent effects. There are several reports on the relationship between the IGF axis and HCC.[29-31] IGFBP-3 is the most abundant IGFBP present in noncancerous liver tissue and could serve as a negative regulator of cell proliferation in human HCCs.[32] Although the presence of IGFBP-5 in numerous tumors and cell lines has been demonstrated, its expression and significance in human HCC have not been documented. We found positive staining for IGFBP-5 in 42% of HCCs, and the positivity correlated with absence of portal venous invasion, low TNM stage, and small tumor size. Although not statistically significant, patients with IGFBP-5–positive HCCs tended to survive longer than those with IGFBP-5–negative HCCs. These findings are essentially similar to those observed for gankyrin. Regarding the effect of IGFBP-5 on cell proliferation, there are contradictory findings.[28] In breast cancer cells, many studies have reported inhibition of growth, but there are some indicating a stimulatory effect.[33] IGFBP-5 is up-regulated in involuting prostate but is also implicated in growth stimulation of prostate tumor cells.[34] We found that down-regulation of IGFBP-5 suppresses growth of Huh-7 HCC cells. Thus, these findings are consistent with a notion that high expression of IGFBP-5 and gankyrin play oncogenic roles in HCCs of early clinical stages. Clarification of the exact roles played by them will shed more light on the molecular mechanisms of human hepatocarcinogenesis and lead to development of new therapeutic and preventive strategies.

Acknowledgment: We thank Dr. R. John Mayer for helpful suggestions.

References

1. Parkin DM, Bray F, Ferlay J, Pisani P. Global cancer statistics, 2002. CA Cancer J Clin 2005;55:74-108.
2. Thomas MB, Zhu AX. Hepatocellular carcinoma: the need for progress. J Clin Oncol 2005;23:2892-2899.
3. Treiber G, Wex T, Rocken C, Fostitsch P, Malfertheiner P. Impact of biomarkers on disease survival and progression in patients treated with octreotide for advanced hepatocellular carcinoma. J Cancer Res Clin Oncol 2006;132:699-708.
4. Shimada K, Sano T, Sakamoto Y, Kosuge T. A long-term follow-up and management study of hepatocellular carcinoma patients surviving for 10 years or longer after curative hepatectomy. Cancer 2005;104:1939-1947.
5. Poon RT, Fan ST, Ng IO, Lo CM, Liu CL, Wong J. Different risk factors and prognosis for early and late intrahepatic recurrence after resection of hepatocellular carcinoma. Cancer 2000;89:500-507.
6. Kiyosawa K, Umemura T, Ichijo T, Matsumoto A, Yoshizawa K, Gad A, et al. Hepatocellular carcinoma: recent trends in Japan. Gastroenterology 2004;127(5 Suppl 1):S17-S26.
7. Higashitsuji H, Higashitsuji H, Nagao T, Nonoguchi K, Fujii S, Itoh K, et al. A novel protein overexpressed in hepatoma accelerates export of NF-kappa B from the nucleus and inhibits p53-dependent apoptosis. Cancer Cell 2002;2:335-346.
8. Gotoh K, Nonoguchi K, Higashitsuji H, Kaneko Y, Sakurai T, Sumitomo Y, et al. Apg-2 has a chaperone-like activity similar to Hsp110 and is overexpressed in hepatocellular carcinomas. FEBS Lett 2004;560:19-24.
9. Higashitsuji H, Itoh K, Nagao T, Dawson S, Nonoguchi K, Kido T, et al. Reduced stability of retinoblastoma protein by gankyrin, an oncogenic ankyrin-repeat protein overexpressed in hepatomas. Nat Med 2000;6:96-99.
10. Higashitsuji H, Liu Y, Mayer RJ, Fujita J. The oncoprotein gankyrin negatively regulates both p53 and RB by enhancing proteasomal degradation. Cell Cycle 2005;4:1335-1337.
11. Hori T, Kato S, Saeki M, DeMartino GN, Slaughter CA, Takeuchi J, et al. cDNA cloning and functional analysis of p28 (Nas6p) and p40.5 (Nas7p),

two novel regulatory subunits of the 26S proteasome. Gene 1998;216:113-122.
12. Dawson S, Apcher S, Mee M, Higashitsuji H, Baker R, Uhle S, et al. Gankyrin is an ankyrin-repeat oncoprotein that interacts with CDK4 kinase and the S6 ATPase of the 26 S proteasome. J Biol Chem 2002;277: 10893-10902.
13. Li J, Tsai MD. Novel insights into the INK4-CDK4/6-Rb pathway: counter action of gankyrin against INK4 proteins regulates the CDK4-mediated phosphorylation of Rb. Biochemistry 2002;41:3977-3983.
14. Shan YF, Zhou WP, Fu XY, Yan HX, Yang W, Liu SQ, et al. The role of p28GANK in rat oval cells activation and proliferation. Liver Int 2006;26: 240-247.
15. Iwai A, Marusawa H, Kiuchi T, Higashitsuji H, Tanaka K, Fujita J, et al. Role of a novel oncogenic protein, gankyrin, in hepatocyte proliferation. J Gastroenterol 2003;38:751-758.
16. Higashitsuji H, Higashitsuji H, Itoh K, Sakurai T, Nagao T, Sumitomo Y, et al. The oncoprotein gankyrin binds to MDM2/HDM2, enhancing ubiquitylation and degradation of p53. Cancer Cell 2005;8:75-87.
17. Ueno S, Tanabe G, Nuruki K, Hamanoue M, Komorizono Y, Oketani M, et al. Prognostic performance of the new classification of primary liver cancer of Japan (4th edition) for patients with hepatocellular carcinoma: a validation analysis. Hepatol Res 2002;24:395-403.
18. Desmet VJ. Histological classification of chronic hepatitis. Acta Gastroenterol Belg 1997;60:259-267.
19. Fu XY, Wang HY, Tan L, Liu SQ, Cao HF, Wu MC. Overexpression of p28/gankyrin in human hepatocellular carcinoma and its clinical significance. World J Gastroenterol 2002;8:638-643.
20. Tan L, Fu XY, Liu SQ, Li HH, Hong Y, Wu MC, et al. Expression of p28GANK and its correlation with RB in human hepatocellular carcinoma. Liver Int 2005;25:667-676.
21. Yeoh EJ, Ross ME, Shurtleff SA, Williams WK, Patel D, Mahfouz R, et al. Classification, subtype discovery, and prediction of outcome in pediatric acute lymphoblastic leukemia by gene expression profiling. Cancer Cell 2002;1:133-143.
22. Park TJ, Kim HS, Byun KH, Jang JJ, Lee YS, Lim IK. Sequential changes in hepatocarcinogenesis induced by diethylnitrosamine plus thioacetamide in Fischer 344 rats: induction of gankyrin expression in liver fibrosis, pRB degradation in cirrhosis, and methylation of p16(INK4A) exon 1 in hepatocellular carcinoma. Mol Carcinog 2001;30:138-150.
23. Tanaka S, Toh Y, Adachi E, Matsumata T, Mori R, Sugimachi K. Tumor progression in hepatocellular carcinoma may be mediated by p53 mutation. Cancer Res 1993;53:2884-2887.
24. Hayashi H, Sugio K, Matsumata T, Adachi E, Takenaka K, Sugimachi K. The clinical significance of p53 gene mutation in hepatocellular carcinomas from Japan. HEPATOLOGY 1995;22:1702-1707.
25. Nagao T, Kondo F, Sato T, Nagato Y, Kondo Y. Immunohistochemical detection of aberrant p53 expression in hepatocellular carcinoma: correlation with cell proliferative activity indices, including mitotic index and MIB-1 immunostaining. Hum Pathol 1995;26:326-333.
26. Anzola M, Saiz A, Cuevas N, Lopez-Martinez M, Martinez de Pancorbo MA, Burgos JJ, et al. High levels of p53 protein expression do not correlate with p53 mutations in hepatocellular carcinoma. J Viral Hepat 2004;11: 502-510.
27. Endo K, Ueda T, Ohta T, Terada T. Protein expression of MDM2 and its clinicopathological relationships in human hepatocellular carcinoma. Liver 2000;20:209-215.
28. Beattie J, Allan GJ, Lochrie JD, Flint DJ. Insulin-like growth factor-binding protein-5 (IGFBP-5): a critical member of the IGF axis. Biochem J 2006;395:1-19.
29. Gong Y, Cui L, Minuk GY. The expression of insulin-like growth factor binding proteins in human hepatocellular carcinoma. Mol Cell Biochem 2000;207:101-104.
30. Scharf JG, Dombrowski F, Ramadori G. The IGF axis and hepatocarcinogenesis. Mol Pathol 2001;54:138-144.
31. Breuhahn K, Longerich T, Schirmacher P. Dysregulation of growth factor signaling in human hepatocellular carcinoma. Oncogene 2006;25:3787-3800.
32. Huynh H, Chow PK, Ooi LL, Soo KC. A possible role for insulin-like growth factor-binding protein-3 autocrine/paracrine loops in controlling hepatocellular carcinoma cell proliferation. Cell Growth Differ 2002;13: 115-122.
33. McCaig C, Perks CM, Holly JM. Intrinsic actions of IGFBP-3 and IGFBP-5 on Hs578T breast cancer epithelial cells: inhibition or accentuation of attachment and survival is dependent upon the presence of fibronectin. J Cell Sci 2002;115:4293-4303.
34. Miyake H, Pollak M, Gleave ME. Castration-induced up-regulation of insulin-like growth factor binding protein-5 potentiates insulin-like growth factor-I activity and accelerates progression to androgen independence in prostate cancer models. Cancer Res 2000;60:3058-3064.

RESEARCH ARTICLES

ERK5 is a Target for Gene Amplification at 17p11 and Promotes Cell Growth in Hepatocellular Carcinoma by Regulating Mitotic Entry

Keika Zen,[1] Kohichiroh Yasui,[1]* Tomoaki Nakajima,[1] Yoh Zen,[2] Kan Zen,[3] Yasuyuki Gen,[1] Hironori Mitsuyoshi,[1] Masahito Minami,[1] Shoji Mitsufuji,[1] Shinji Tanaka,[4] Yoshito Itoh,[1] Yasuni Nakanuma,[2] Masafumi Taniwaki,[5] Shigeki Arii,[4] Takeshi Okanoue,[1] and Toshikazu Yoshikawa[1]

[1]Molecular Gastroenterology and Hepatology, Graduate School of Medical Science, Kyoto Prefectural University of Medicine, Kyoto, Japan
[2]Department of Human Pathology, Kanazawa University Graduate School of Medicine, Kanazawa, Japan
[3]Division of Cardiovascular Medicine, Omihachiman Community Medical Center, Omihachiman, Japan
[4]Department of Hepato-Biliary-Pancreatic Surgery, Tokyo Medical and Dental University, Tokyo, Japan
[5]Molecular Hematology and Oncology, Graduate School of Medical Science, Kyoto Prefectural University of Medicine, Kyoto, Japan

Using high-density oligonucleotide microarrays, we investigated DNA copy-number aberrations in cell lines derived from hepatocellular carcinomas (HCCs) and detected a novel amplification at 17p11. To identify the target of amplification at 17p11, we defined the extent of the amplicon and examined HCC cell lines for expression of all seven genes in the 750-kb commonly amplified region. Mitogen-activated protein kinase (MAPK) 7, which encodes extracellular-regulated protein kinase (ERK) 5, was overexpressed in cell lines in which the gene was amplified. An increase in *MAPK7* copy number was detected in 35 of 66 primary HCC tumors. Downregulation of *MAPK7* by small interfering RNA suppressed the growth of SNU449 cells, the HCC cell line with the greatest amplification and overexpression of *MAPK7*. ERK5, phosphorylated during the G2/M phases of the cell cycle, regulated entry into mitosis in SNU449 cells. In conclusion, our results suggest that *MAPK7* is likely the target of 17p11 amplification and that the ERK5 protein product of *MAPK7* promotes the growth of HCC cells by regulating mitotic entry.

INTRODUCTION

Hepatocellular carcinoma (HCC) is the fifth most common malignancy in the world and is estimated to cause approximately half a million deaths annually (El-Serag, 2002). Several risk factors for HCC have been reported, including infection with hepatitis B and C viruses, dietary intake of afratoxin, alcohol consumption, and diabetes.

The mitogen-activated protein kinase (MAPK) cascades transmit extracellular signals from cell surface receptors to specific intracellular targets and regulate a wide variety of cellular functions, including cell proliferation, differentiation, and the stress response (Nishimoto and Nishida, 2006). Extracellular stimuli induce sequential activation of MAPK kinase kinase, MAPK kinase, and MAPK. At least four MAPK subfamilies have been identified: extracellular-regulated protein kinase (ERK) 1 and 2, c-Jun-N-terminal kinases, p38, and ERK5 (also know as BMK1). ERK5, which was recently characterized, can be activated by a wide range of growth factors and cellular stresses, including serum, epithelial growth factor, oxidative stress, and hyperosmotic shock (Hayashi and Lee, 2004; Nishimoto and Nishida, 2006; Wang and Tournier, 2006). When stimulated, MAP/ERK kinase kinase 2 and 3 activate MAP/ERK kinase (MEK) 5, a specific kinase for ERK5. Subsequently, MEK5 phosphorylates ERK5, and the activated ERK5 promotes cell proliferation, differentiation, and survival (Hayashi and Lee, 2004; Garaude et al., 2006; Nishimoto and Nishida, 2006; Wang and Tournier, 2006). Some investigators have described the possible involvement of ERK5 in cancers (Esparis-Ogando et al., 2002; Weldon et al., 2002; Mulloy et al., 2003; Carvajal-Vergara et al., 2005; Linnerth et al., 2005).

Additional Supporting Information may be found in the online version of this article.

Supported by: Grants-in-Aid for Scientific Research from the Japan Society for the Program of Science, Grant number: 18390223.

*Correspondence to: Kohichiroh Yasui, Molecular Gastroenterology and Hepatology, Graduate School of Medical Science, Kyoto Prefectural University of Medicine, 465 Kajii-cho, Kamigyo-ku, Kyoto, 602-8566, Japan. E-mail: yasuik@koto.kpu-m.ac.jp

Received 24 May 2008; Accepted 11 September 2008
DOI 10.1002/gcc.20624
Published online 30 October 2008 in Wiley InterScience (www.interscience.wiley.com).

Accumulating evidence suggests that multiple sequential genetic alterations in a cell lineage at the nucleotide and chromosome levels underlie the carcinogenesis of solid tumors. Amplification of chromosomal DNA is one mechanism of activating genes whose overexpression contributes to the development and progression of cancer. Regions of chromosomal amplification in cancer cells frequently harbor oncogenes, such as *MYC* (Little et al., 1983) and *ERBB2* (Di Fiore et al., 1987). Using comparative genomic hybridization (CGH), we have detected novel regions of amplification in a variety of cancer types, including HCC, and we have identified a number of candidate oncogenes from amplicons (Yasui et al., 2001; Yasui et al., 2002; Yokoi et al., 2002; Okamoto et al., 2003; Yokoi et al., 2003). CGH was initially used for genome-wide detection of copy number changes occurring in cancers (Kallioniemi et al., 1992). However, its resolution is limited (5–10 Mb) because it detects segmental copy number changes on metaphase chromosomes.

The recent introduction of high-density oligonucleotide microarrays designed for typing of single nucleotide polymorphisms (SNPs) facilitates high-resolution mapping of chromosomal amplifications, deletions, and loss of heterozygosity (Mei et al., 2000; Bignell et al., 2004; Matsuzaki et al., 2004a,b; Wong et al., 2004; Zhao et al., 2004). The Affymetrix GeneChip Mapping 100K array set contains 116,204 SNP loci with a mean intermarker distance of 23.6 kb, and it enables detailed and genome-wide identification of DNA copy number changes (Matsuzaki et al., 2004a,b; Garraway et al., 2005; Zhao et al., 2005). The newer GeneChip Mapping 500K array set is composed of two arrays, each capable of genotyping an average 250,000 SNPs.

In the work reported here, we investigated DNA copy number aberrations in HCC cell lines using Affymetrix high-density SNP arrays. We identified a novel amplification at 17p11 in HCC cell lines. This region may harbor one or more genes that, when amplified, contribute to carcinogenesis. Within the amplicon, *MAPK7*, which encodes ERK5, emerged as a probable target gene that acts as a driving force for amplification of the region and promotes the growth of HCC cells by regulating entry into mitosis.

MATERIALS AND METHODS

Cell Lines and Tumor Samples

A total of 21 liver cancer cell lines [HCC-derived HLE, HLF (Dor et al., 1975), PLC/PRF/5 (Alexander et al., 1976), Li7 (Hirohashi et al., 1979), Huh7 (Nakabayashi et al., 1982), Hep3B (Aden et al., 1979), SNU354, SNU368, SNU387, SNU398, SNU423, SNU449, SNU475 (Park et al., 1995), JHH-1, JHH-2, JHH-4, JHH-5, JHH-6, JHH-7 (Fujise et al., 1990), Huh-1 (Huh et al., 1981), and the hepatoblastoma line HepG2 (Knowles et al., 1980)] were examined in this study. All cell lines were maintained in Dulbecco's modified Eagle's medium supplemented with 10% fetal bovine serum. We obtained 66 primary HCC tumors for analysis of the DNA copy number of *MAPK7* from patients undergoing surgery at the hospitals of Tokyo Medical and Dental University and Kyoto University, Japan. Genomic DNA was isolated from each cell line and from 66 primary tumors using the Puregene DNA isolation kit (Gentra, Minneapolis, MN). For immunohistochemical studies of ERK5, 43 additional HCC samples were obtained from the Hospital of Kyoto Prefectural University of Medicine, Japan. Before initiation of the present study, informed consent was obtained in the formal style approved by all relevant ethical committees.

SNP Assay

The GeneChip Mapping 100K array set and GeneChip Mapping 250K Sty array (Affymetrix, Santa Clara, CA) were used in this study. Analyses were performed according to the manufacturer's instructions. In brief, 250 ng of genomic DNA was digested with a restriction enzyme (*Xba*I or *Hind*III for the 100K array set and *Sty*I for the 250K Sty array), ligated to an adaptor, and amplified by PCR (Kennedy et al., 2003; Matsuzaki et al., 2004a,b; Zhao et al., 2004). Amplified products were fragmented, labeled by biotinylation, and hybridized to the microarrays. Hybridization was detected by incubation with a streptavidin-phycoerythrin conjugate, followed by scanning of the array, and analysis was performed as described previously (Kennedy et al., 2003; Di et al., 2005). Copy number changes were calculated using the Copy Number Analyzer for Affymetrix GeneChip Mapping Arrays (http://www.genome.umin.jp) (Nannya et al., 2005).

Fluorescence In Situ Hybridization

We performed FISH using the bacterial artificial chromosome (BAC) RP11-73E4 as a probe (Invitrogen, Carlsbad, CA) as described previously (Yasui et al., 2002). The BAC was selected

on the basis of its location according to the database provided by the UCSC (http://genome.ucsc.edu/). Briefly, the probe was labeled by nick translation with biotin-16-dUTP (Roche Diagnostics, Penzberg, Germany) and hybridized to metaphase chromosomes. Hybridization signals for biotin-labeled probes were detected with avidin-fluorescein (Roche Diagnostics).

Real-Time Quantitative PCR

We quantified genomic DNA and mRNA using a real-time fluorescence detection method. Total RNA was obtained using Trizol (Invitrogen). Residual genomic DNA was removed by incubating the RNA samples with RNase-free DNase I (Takara Bio, Shiga, Japan) prior to reverse transcription (RT)-PCR. Single-stranded complementary DNA was generated using superscript III reverse transcriptase (Invitrogen) according to the manufacturer's directions. Real-time quantitative PCR experiments were performed with the LightCycler system using FastStart DNA Master Plus SYBR Green I (Roche Diagnostics) according to the manufacturer's protocol. The primers were as follows: *MAPK7* DNA (forward, 5′-TGCTGACTGGCTCGAAG-3′; reverse, 5′-GGGTCTGAGATGAACCTGC-3′); *MAPK7* mRNA (forward, 5′-TTTGCCTTACTTCCCACCTG-3′; reverse, 5′-CCCATGTCGAAAGACTGGTT-3′); *GRAP* mRNA (forward, 5′-TCGAAGGACAGACTGCACAC-3′; reverse, 5′-AGAAGAGGAGTGTGCCTCCA-3′); *EPN2* mRNA (forward, 5′-TCACCTCACCCACCACTGTA-3′; reverse, 5′-GTGGTCAGCTGCCCTTAGAG-3′); *EPPB9* mRNA (forward, 5′-CTTTGTGTACGGCCAGGACT-3′; reverse, 5′-CGTAGGGGTTGGTGCTTTTA-3′); *MFAP4* mRNA (forward, 5′-GGTGACTCCCTGTCCTACCA-3′; reverse, 5′-TCATCTCAGTGCGTTTGAGG-3′); *ZNF179* mRNA (forward, 5′-ACTGGGCAGAACCAGAGAGA-3′; reverse, 5′-AGGATGCACAGACAGGCTCT-3′); *FLJ10847* mRNA (forward, 5′-AACTCTTGGGCTTCAAGCAA-3′; reverse, 5′-AGGAGGTTGAGGCTGCAGTA -3′). These primers were designed using Primer3 (http://frodo.wi.mit.edu/cgi-bin/primer3/primer3_www.cgi) on the basis of sequence data obtained from the NCBI database (http://www.ncbi.nlm.nih.gov/). *GAPDH* (Minamiya et al., 2004) and long interspersed nuclear element (LINE)-1 (Zhao et al., 2004) were used as endogenous controls for mRNA and genomic DNA levels, respectively.

Immunoblotting

Immunoblots were prepared according to previously reported methods (Yasui et al., 2001). Cell lysates (20 μg protein per sample) were separated by sodium dodecyl sulfate-polyacrylamide gel electrophoresis on 10% acrylamide gels. We obtained the following antibodies from Sigma-Aldrich (Tokyo, Japan): anti-ERK5 polyclonal antibody, anti-phospho-ERK5 (pThr218/pThr220) polyclonal antibody, and anti-β-actin monoclonal antibody. For immunoblotting, we used anti-ERK5, anti-phospho-ERK5, and anti-β-actin at dilutions of 1:500, 1:1000, and 1:5000, respectively. For secondary immunodetection, we used anti-rabbit or anti-mouse Ig (Amersham, Tokyo, Japan) diluted 1:5000. Protein binding was detected using the ECL system (Amersham).

Immunoprecipitation

Cells were lysed with RIPA buffer (10 mM Tris-HCl, pH 7.4, 150 mM NaCl, 1% Triton X-100, 0.1% sodium dodecyl sulfate, 1% sodium deoxycholate, 1 mM phenylmethylsulfonyl fluoride), and incubated on ice for 30 min. The lysate was centrifuged at 14,000 × *g* at 4°C for 15 min. The supernatant was incubated with normal rabbit IgG and protein A-agarose beads (Santa Cruz Biotechnology, Santa Cruz, CA) to decrease nonspecific protein binding. After centrifugation, the supernatant was incubated with anti-ERK5 polyclonal antibody or normal rabbit IgG (control) overnight at 4°C. Protein A-agarose beads were added to the reaction and the mixture was incubated for an additional 1 hr. The precipitates were recovered by a brief centrifugation, followed by four washes with RIPA buffer. Samples were then boiled in electrophoresis sample buffer and separated by electrophoresis as described above (see "Immunoblotting" section).

Immunohistochemical Analysis

Forty-three primary HCCs, consisting of paired tumor and surrounding nontumor tissues, and two HCC cell lines (SNU449 and Li7) were analyzed by anti-ERK5 immunostaining. Immunohistochemical staining was performed on formalin-fixed and paraffin-embedded sections using an anti-ERK5 polyclonal antibody (Sigma-Aldrich) at a 1:200 dilution. An automated tissue immunostainer (Ventana Medical Systems, Tucson, AZ) was used according to the manufacturer's instructions. The staining was developed with 3,3′-

diaminobenzidine tetrahydrochloride, followed by counterstaining with hematoxylin.

Growth Assays and RNA Interference Studies

For cell growth assays viable cells were stained with 0.2% trypan blue and counted with a hemocytometer 24, 48, and 72 hr after transfection. For RNA interference (RNAi) studies, Stealth small interfering RNA (siRNA) duplex oligoribonucleotides targeting *MAPK7* (5′-CCAUGGCAUGAAC CCUGCCGAUAUU-3′) and Stealth RNAi negative control duplexes were synthesized by Invitrogen. The siRNAs were delivered into SNU449 cells using Lipofectamine 2000 (Invitrogen) according to the manufacturer's instructions. To determine mRNA levels, cells were harvested 48 hr after transfection and subjected to quantitative RT-PCR as described above.

Cell Cycle Synchronization

SNU449 cells were synchronized at G1/S, early S, or M phases. For G1/S or early S-phase synchronization, cells were incubated in medium containing 2.5 mM thymidine (Sigma Chemical Co., St. Louis, MO) for 24 hr, followed by 12 hr in medium without thymidine, and finally another 12 hr in medium containing 2.5 mM thymidine (double-thymidine block; for G1/S-phase) or 1 μg/ml aphidicolin (early S-phase block). For M phase synchronization, cells were incubated in medium containing 2.5 mM thymidine for 24 hr, followed by 4 hr in medium without thymidine, and finally another 12 hr in medium containing 0.5 μg/ml nocodazole.

Cell Cycle Analysis

SNU449 cells were synchronized at the G1/S-phase boundary by a double-thymidine block as described above. Synchronized cells were released into fresh medium without thymidine and harvested at the indicated time points. These cells were then stained with propidium iodide and analyzed using a FACSCaliber scanner and Cell Quest software (Becton Dickinson Pharmingen, San Diego, CA).

Mitotic Index

Cells were grown in 24-well plates and transfected with Stealth RNAi targeting *MAPK7* or Stealth RNAi negative control duplexes as described above (see "Growth Assays and RNA Interference Studies" section). After 24 hr, cells were synchronized at the G1/S-phase boundary by a double-thymidine block. Synchronized cells were collected, reseeded on glass slides, and incubated for an additional 9 hr in fresh medium without thymidine. Next, the cells were stained with an anti-phospho-histone H3 antibody that specifically detects mitotic cells. Briefly, cells were fixed with 3.7% formaldehyde, permeabilized with 0.25% Triton X-100, and incubated with PBS containing 1% bovine serum albumin. The cells were then treated with a mixture of 4 μg/ml anti-phospho-histone H3 (Ser10)-biotin conjugated antibody (Upstate Biotechnology, Lake Placid, NY) and a 1:100 dilution of streptavidin-fluorescein (Roche Diagnostics) for 1 hr at room temperature, followed by counterstaining with propidium iodide. Positive staining for phospho-histone H3 was quantified by counting stained cells under a fluorescence microscope and dividing by the number of total cells. The mitotic index was scored as the percentage of mitotic cells in a population. On average, 200 cells were scored in three separate areas.

Statistical Analysis

All statistical analyses were performed using SPSS 15.0 software (SPSS Inc., Chicago, IL). Chi-square tests or analysis of variance (ANOVA) were used. P values < 0.05 were considered significant.

RESULTS

Detection of the 17p11 Amplicon in HCC Cell Lines by SNP Array Analysis

We screened for DNA copy number aberrations in 20 HCC cell lines by SNP array analysis. Two of the 20 cell lines, SNU449 and JHH-7, exhibited amplifications at chromosomal band 17p11 (Fig. 1A). In particular, the SNU449 cell line showed a high level of amplification in a narrow region on 17p11. We were able to define the smallest commonly affected region in the 17p11 amplicon as that lying between the positions recognized by the Affymetrix SNP_A-1662618 and SNP_A-1720748 probes (Fig. 1B). This region includes seven known or predicted protein-coding genes, *GRAP*, *EPN2*, *EPPB9*, *MAPK7*, *MFAP4*, *ZNF179*, and *FLJ10847*. The size of the amplicon was estimated to be approximately 750 kb.

To confirm amplification at 17p11 in SNU449 cells, we performed FISH analysis. The probe for